Biomaterials Science

Toward Reducing Biomaterials Antigenic Potential: A Miniaturized Fc-Binding Domain for Local Deposition of Antibodies

Journal:	*Biomaterials Science*
Manuscript ID	BM-ART-10-2018-001220.R2
Article Type:	Paper
Date Submitted by the Author:	14-Nov-2018

Complete List of Authors:	Pham, Ngoc; Duquesne University, Graduate School of Pharmaceutical Sciences Liu, Wen; Duquesne University, Graduate School of Pharmaceutical Sciences Schueller, Nathan; Duquesne University, Graduate School of Pharmaceutical Sciences Gawalt, Ellen; Duquesne University, Department of Chemistry and Biochemistry Fan, Yong; Allegheny-Singer Research Institute, Institute of Cellular Therapeutics Meng, Wilson; Duquesne University, Graduate School of Pharmaceutical Sciences

Toward Reducing Biomaterials Antigenic Potential: A Miniaturized Fc-Binding Domain for Local Deposition of Antibodies

Ngoc B. Pham[‡], Wen Liu[‡], Nathan R. Schueller[‡], Ellen S. Gawalt[¶⌋], Yong Fan[ǂ§], and Wilson S. Meng[‡⌋*]

[‡]Graduate School of Pharmaceutical Sciences, [¶]Department of Chemistry and Biochemistry, Duquesne University, Pittsburgh, PA 15282, USA

[ǂ]Institute of Cellular Therapeutics, Allegheny-Singer Research Institute, Allegheny Health Network, Pittsburgh, PA 15212, USA

[§]Department of Biological Sciences, Carnegie-Mellon University, Pittsburgh, PA 15213, USA

[⌋]McGowan Institute for Regenerative Medicine, University of Pittsburgh, PA 15213, USA

Key words: Protein A, EAK, drug delivery, controlled release, self-assembling peptide, hydrogel

***Corresponding author**: Wilson Meng, Ph.D., Graduate School of Pharmaceutical Sciences, Duquesne University, 600 Forbes Avenue, Pittsburgh, PA 15282; Tel: 1-(412)-396-6366; Fax: 1-(412)-396-4660; E-mail: meng@duq.edu

Abstract

A peptide derived from Staphylococcal Protein A (SpA) was developed as an affinity module for antibody delivery applications. The miniaturized protein consists of the first helix of the engineered SpA Z domain fused with the self-assembling peptide (SAP) AEAEAKAKAEAEAKAK, or EAK. The resulting peptide, named Z15_EAK, was shown to possess fibrillizing property and Fc-binding function. The peptide induced a red shift in the Congo red absorbance characteristic of peptide fibrils, also evidenced in transmission electron microscopic images. The one-site binding affinity (K_d) of a gel-like coacervate generated by admixing Z15_EAK with EAK for IgG was determined to be 1.27 ± 0.14 μM based on a microplate-based titration assay. The coacervate was found to localize IgG subcutaneously in mouse footpads for 8 to 28 days. A set of *in vivo* data was fit to a one-compartment model for simulating the relative fractions of IgG dissociated from the materials in the depot. The model predicted that close to 27% of the antibody injected were available as unbound for the duration of the experiment. Z15_EAK did not appear to induce innate immune responses; injecting Z15_EAK into mouse footpads elicited neither interleukin-6 (IL-6) nor tumor necrosis factor-alpha (TNF-α) from splenocytes isolated from the animals one day, seven days, or eleven days afterward. The antigenic potential of Z15 was analyzed using a bioinformatic approach in predicting sequences in SpA and Z15 dually presented by class I and class II human MHC alleles covering the majority of the population. A peptide in SpA identified as a potential T cell epitope cross reacting with a known epitope in a microbial antigen was eliminated by the miniaturization. These results demonstrate that Z15_EAK is a potential platform for generating antibody depots by which the impacts of Fc-based biotherapeutics can be enhanced through spatiotemporal control.

Introduction

EAK16-II is a self-assembling peptide (SAP) that has been investigated extensively for developing hydrogel matrices in drug delivery and tissue engineering applications [1-3]. The unique pattern of alternating negative and positive charges interspersed with a small hydrophobic residue in AEAEAKAKAEAEAKAK (referred to as EAK hereafter) drives the peptide to undergo sol-gel phase transition, forming cross-linking β-fibrils in the presence of salt. We have used a coassembly strategy to engineer Fc-binding function into the fibrillar materials by mixing EAK with another EAK-containing peptide appended with a His-tag (EAKH6) or the single-chain variable fragment dL5 (dL5_EAK) [4-11]. These Fc-binding composites can concentrate IgG antibodies locally *in vivo*. The components can be kept soluble in deionized water prior to injecting *in vivo* to initiate coacervation. In these systems, recombinant protein A/G was used as the Fc-binding domain.

Because of its high affinity and specificity, Staphylococcal Protein A (SpA) is used as a purification module for IgG and Fc-fusion proteins in both laboratory and industrial settings [12]. Highly purified SpA at very low doses is also being developed as a therapeutic for idiosyncratic thrombocytopenia purpura in humans; phase-I clinical trials of the SpA (PRTX-100) have shown that the agent is safe [13]. The product is currently being tested in phase II (Clinical Trial.Gov entry: NCT02401061). The use of SpA in biomedical applications is nevertheless limited by the bacterial origin of the protein and its potential immunogenicity in humans because higher doses and repeated injections might be necessary. SpA would contain B-cell epitopes, rendering it a target of neutralizing antibodies, which can negate the protein's antibody-capturing function. SpA would also contain T cell epitopes, therefore can stimulate CD8 cytotoxic T cells (CTLs) by

which cutaneous reactions may occur. Miniaturization of SpA into a small peptide will reduce its immunogenic potential while preserving the affinity for immunoglobulins and Fc-fusion proteins in drug delivery applications.

SpA is a 42-kDa protein consisting of five homologous Fc-binding domains (E, D, A, B and C) [14, 15]. Each domain adopts a three-helix conformation. A smaller variant named "Z38" (14.5 kDa) was derived from the native B domain Generated through phage display randomization and point mutations [12, 16] (Fig. 1a). Crystal structures of SpA B domain and Z38 complexed with IgG and Fc fragments indicate the interactions are concentrated in the first two helices [17-20]. Subsequently Z34c was generated as a disulfide-linked cyclic peptide consisting of two helices making contacts with the Fc CH2-CH3 and Fab regions in IgG [20], analogous to helix-1 and helix-2 of the B domain. The binding constants of Z34c and SpA for IgG are comparable, both at approximately 20 nM. Of the 11 residues making non-covalent bonds with Fc, six are located in the first helix and five are located in the second [17, 18, 20], with overall structure stabilized through a disulfide bond [20]. These insights provided the basis by which Z34c could be miniaturized yet retaining its Fc-binding function. Truncating the polypeptide to a minimal sequence would generate a sequence with fewer T and B cell epitopes. Engineering strategies have been employed for optimizing the physical and biological properties of peptide and protein biomaterials [21-23].

Herein we report a SpA mimetic in Z15, a 15-amino acid sequence encompassing the first helix in which the majority of contacts with IgG-Fc are located [17, 18, 20]. This 1.9 kDa fragment was predicted to exhibit lower antigenic potential compared to SpA, or the two-helix Z34c protein.

Z15 was converted into a biomaterial tool by appending at the C-terminus the EAK sequence (Fig. 1b). The resulting 3.8 kDa peptide is referred to as Z15_EAK hereafter (Fig. 1). The peptide contains two putative functional domains in Fc-binding near the N-terminus and β-fibrillization near the C-terminus. We hypothesized that admixing Z15_EAK with EAK would result in a stable coacervate (Z15_EAK/EAK) by which local retention of IgG could be extended *in vivo* for days. Such system could be effective in enhancing the therapeutic impacts of monoclonal antibodies and Fc fusion proteins.

Methods and Materials

Peptides

Z15_EAK peptide was synthesized by EZBiolab and arrived as lyophilized powder. Z15_EAK peptide was reconstituted in sterile deionized water (HyPure, Hyclone) to 5 mg/ml (1.288 mM). EAK lyophilized peptide (>95% purity) manufactured by American Peptides Company was reconstituted with sterile water to 5mg/ml (3.02 mM). The peptide solutions were stored at -80^{0}C for long-term storage or -20^{0}C for immediate use.

Fluorescence measurements

Congo red dye (1x) was prepared by diluting the 10X stock in phosphate buffer saline (PBS). Peptides were incubated with Congo red for at least 1 hour and scanned for absorption in the 400-600nm range. The measurement was made with a 0ms settle time using a TECAN infinite M1000 microplate reader (Männedorf, Switzerland).

Transmission electronic microscopy

Fibril formation of Z15_EAK peptide was visualized with transmission electronic microscopy. 200 mesh copper grids were coated with Formva resin in dichloromethane and pretreated with bacitricin. Then, the grids were exposed to Z15_EAK (0.05 mg/ml) and PBS (1x). After that, the grids were stained with 1% uranyl acetate that had been filtered through a 0.2um filter. Upon complete drying, the grids were scanned with a JEM-1210 TEM at high voltage (60kV). The photomicrographs were captured with an AMT camera system, and fibril dimension was analyzed using ImageJ (version 1.8.0).

Spectroscopic analyses

Infrared spectroscopy was utilized to gain insight into the secondary structures of Z15_EAK and EAK upon their incorporation. Each peptide reconstituted in water was distributed on a stainless-steel square and evaporated overnight. A background control was prepared with water on the steel square. The peptide spectra were collected under a Diffuse Reflectance Infrared Fourier Transform (DRIFT) mode on a Nexus 470 FT-IR E.S.P at 1024 scans with a defined resolution of 4 cm^{-1}. The spectra were analyzed and presented with OMNIC 8.3.103 and Origin 8 software.

Paper Chromatography

Binding properties of Z15_EAK to IgG were examined under non-equilibrium conditions through a paper chromatography assay. The paper (Whatman, GE Healthcare) was cut to approximately 10x10 cm in area with two horizontal lanes marked 3cm from the bottom of the paper and 3 cm apart. Rabbit anti-Human IgG (H+L) cross-absorbed IgG antibody conjugated with DyLight 800 (Thermo Fischer Scientific, Waltham, MA.), hereafter IgG^{800}, was spotted on

the bottom horizontal line, creating four vertical lanes for antibody migration (2cm distance between lanes). Vertically above the IgG^{800} lanes, peptides or blank medium volume were spotted on the second horizontal line. The bottom of the paper was then immersed in PBS. IgG^{800} was migrated upward by capillary action and interacted with the peptides spotted above. Before the buffer and sample reached the top of the paper, the paper was removed from the buffer reservoir and air-dried. Near-infrared fluorescence of IgG were captured with an Odyssey Imager (Li-Cor, Inc., Lincoln, NE) at a resolution of 169 μm, an intensity of 2.0 with focal distances of 3.2 mm.

Sodium dodecyl sulfate polyacrylamide electrophoresis (SDS-PAGE)

Z15_EAK and EAK at various ratios were incubated in PBS at 37 ℃ overnight. After centrifugation at 16000 rcf, the supernatants were analyzed through an electrophoresis assay with denaturing NuPAGE™ Novex® 4-12% gels (Life Technologies, Carlsbad, CA). Proteins were visualized using the SilverQuest™ staining kit (Life Technologies) with a reported detection limit of 0.3 ng and imaged using the Kodak 440 Image Station (Rochester, NY). Band intensities were quantified using ImageJ (version 1.8.0).

Isothermal Titration Calorimetry

The equilibrium binding constants (K_a and derived K_d) between Z15_EAK and IgG were determined using a MicroCal VP-ITC instrument (Malvern Pananalytical). Rabbit polyclonal IgG (8.33 μM) was placed into the sample cell, followed by 59 (5μl) injections of Z15_EAK (128 μM). In the reference cell, water was used instead of Z15_EAK, followed by IgG addition after degassing for 10 min with stirring. The titration was performed at 25°C. The instrument

detects the heat released or absorbed when Z15_EAK and IgG interact over the titration by measuring the power needed to maintain isothermal conditions between the reference and the sample cells. The data was analyzed with Origin VP-ITC software.

In vitro binding with IgG

Fluorescein (FITC)-labeled rabbit polyclonal anti-human IgG (Life Technologies, Carlsbad, CA), rbIgG-FITC, was used to examine *in vitro* binding with the Z15_EAK/EAK coacervate. The first method was a "pull-down" assay where IgG ($6.6x10^{-6}$ μmol) was incubated with Z15_EAK (0.03 μmol), EAK (0.06 μmol) and PBS in polystyrene micro-centrifuge tubes. After five washing and centrifugation (16,000g) steps, the gel was recovered and scanned for IgG fluorescence intensity. In the second assay, varying molar concentrations of IgG were titrated against a fixed quantity of Z15_EAK/EAK in Corning 96-well Solid Black Round-bottom Microplates (Fisher Scientific). A repeated process of washing and centrifugation was done to remove unbound antibodies using Wash Buffer (0.05% Tween20 in PBS) followed by 4000 rpm for 2 minutes. Fluorescence intensities of rbIgG-FITC were determined by Victor^3 1420 Multilabel Counter (PerkinElmer, Waltham, MA). K_d values of the antibody and the peptide coacervate interaction were estimated through one-site specific binding at saturation analysis in GraphPad Prism 5.0.

In vivo IgG tracking

Eight to twelve-week old female C57BL/6 mice were purchased from Hilltop laboratory Animals (Scottdale, PA) and housed in the Duquesne University Animal Care Facility. The facility is registered as a research facility with the USDA (23-R-013) and has a Letter of Assurance on file

with United States Office of Laboratory Animal Welfare (Assurance No. A4009-01). All animal experiments were conducted according to the guidelines specified in the U.S. Animal Welfare Act (AWA) and the United States Public Health Service Policy on Humane Care and Use of Laboratory Animals (commonly known as PHS Policy). All animal use protocols were approved by Duquesne University Institutional Animal Care & Use Committee (IACUC). Anesthetization was induced using isoflurane (induction 5%, maintenance 3%) for real time *in vivo* imaging. Hairs at the region of interest were removed prior to sample injection and imaging; this step was omitted in footpad injection. Latex-free syringes with 28G1/2 needles were used to subcutaneously inject Rabbit anti-Human IgG (H+L) cross-absorbed antibody conjugated with DyLight 800 (Thermo Fisher Scientific), hereafter IgG^{800}, with or without the peptide coacervate. Mice were scanned prior to injection and monitored at the indicated times after injection using a Pearl Impulse imager (Li-Cor, Inc.). All images in each set of experiment were collected using the same threshold and resolution (255 μm) settings. Oval-shaped regions of interest were defined at the site of injection and a non-injected site on the body as background. Fluorescence intensities were quantified using the Impulse (2.0) software (Li-Cor, Inc.). *Ex vivo* image was obtained with Li-Cor Odyssey (800-channel, 169 μm resolution, 3.2mm focus offset). *Ex vivo* fluorescence intensity was quantified with Image Studio Lite software 5.2 (Li-Cor, Inc.).

Modeling and simulations

Matlab 2017b with a Simbiology module was utilized to simulate concentration of unbound IgG upon footpad injection with Z15_EAK/EAK. *In vivo* near-infrared signal intensities over 28 days were quantified and converted to concentrations using the intensity obtained 5 minutes after injection as the initial IgG^{800} dose (0.065 μg/μl). A one-compartment model was built assuming

the reversible association between IgG and gel materials and only unbound IgG can leave the footpad compartment (first-order). The volume of injection (50 μL) was designated as the volume of the depot compartment. From *in vitro* data, IgG dissociates from Z15_EAK/EAK with the K_d at approximately 1μM, thus the initial k_{off} and k_{on} values were set as 0.015 (day^{-1}) and 1 ($(\mu g/\mu l)^{-1} \cdot day^{-1}$). *In vivo* footpad IgG concentrations were fitted into the first order decay model to estimate kinetic parameters (k_{on}, k_{off}, k_{el}). These parameters were then incorporated into the one-compartment model to simulate the unbound IgG concentration over time at different dosing regimens. The model was governed by the following differential equations and reactions:

$$\frac{d(Ab_{Z15EAK})}{dt} = \frac{1}{depot * (-reaction_1)}$$

$$\frac{d(Ab)}{dt} = \frac{1}{depot * (-reaction_1 - reaction_2)}$$

$$\frac{d(Z15EAK)}{dt} = \frac{1}{depot * (reaction_1)}$$

$$reaction_1 = k_{off} * Ab_{Z15EAK} - k_{on} * Ab * Z15EAK$$

$$reaction_2 = k_{el} * Ab$$

Inflammation evaluation

Ex vivo inflammation stimulation was done by incubating naïve splenocytes with 1 or 10 μg of Z15_EAK in 1 ml of media. After 48 hours, a mouse IL-6 ELISA kit (BD OptEIA Mouse IL-6 ELISA kit, limit of quantification, or LOQ, of 15.6 pg/mL) was used to evaluate if the peptide interacted with splenocytes and generated pro-inflammatory cytokine. *In vivo* inflammation evaluation was done by subcutaneously injecting 125-250 μg of Z15_EAK to C57BL/6 mouse footpads. At different time points (1, 7, and 11 day(s)) mice were euthanized and spleens were isolated. After removal of red blood cells using a hypotonic buffer, the leukocytes were cultured overnight, and the supernatants were assayed for mouse IL-6 (BD OptEIA Mouse IL-6 ELISA kit, LOQ = 15.6 pg/mL) and TNFα (Invitrogen Mouse TNFα ELISA Ready-Set-Go, LOQ = 8 pg/mL). The mice were observed for weight loss, signs of swelling and redness. In the 7-day experiment, 125 μg (in 25μl) Z15_EAK was injected into the right footpad whereas the left footpad received 25 μl saline. The footpad thickness was measured with a digital caliper before, 2 min, 1 h and 7 days after injection.

Statistical analysis

Statistical analysis was performed in GraphPad Prism 5.0. Data shown represent mean and standard mean error. *In vitro* pull-down assay data was analyzed with an unpaired t-test, $p < 0.05$. IgG titration study was fitted to a nonlinear regression one-site specific binding curve fit and reported with 95% confidence interval. *In vivo* fluorescence intensities were analyzed with Two-way ANOVA and a Bonferroni's method for multiple comparison of intensity means at each time point ($p<0.001$ and $p<0.01$).

Results

The Z15 sequence traced back to SpA through Z38 and Z34c (Fig. 1a). Starting from the native B domain of SpA, Z38 was generated through substitutions and truncation, preserving 23 amino acids of the first two helices [24]. The Fc-binding domain was modified in Z34c in which a pair of cysteine residues was introduced near the N and C termini, thereby constraining the conformation into a stable two-helix structure [20]. We hypothesized that Fc binding would be preserved by isolating the first helix in which six of the eleven interactions are located. Hence, the SAP EAK was appended to the first 15 amino acids of Z34c (with the cysteine replaced with an alanine) to generate Z15_EAK (Fig. 1b) as a module by which EAK β-fibrils could be functionalized for capturing immunoglobulins.

Physical properties of Z15_EAK

We first determined the extent to which the two domains in Z15_EAK retained their functional properties (Fig. 2). The fibrillization potential of Z15_EAK was characterized by adding the peptide to a phosphate buffer saline solution of Congo red (Fig. 2a). This resulted in a red shift of a peak absorbance (from 490 nm to 500 nm), which is a characteristic of binding of the dye to β-fibrils, with the initial microstructures appearing after 3 hours of incubation (Fig. 2b). TEM images further indicated that Z15_EAK could form fibrils independent of EAK (Fig. 2c). Fibrils as long as 1 μm could be seen, with average widths fell in two populations, 56.3 ± 18.1 nm and 28.3 ± 8.18 nm, together forming a cross-linking network similar to those observed in EAK samples [2]. These observations were unexpected as EAKH6 [5] and dL5_EAK [9] do not undergo β-fibril self-assembly. The propensity for Z15_EAK to self-assemble into β-fibrils was further supported by the peaks at 1613 nm, and amide-I (1698 nm) and amide-II (1551 nm) detected in infrared spectroscopy (Fig. 2d). The peak 1638 nm was assigned as α-helix, presumably

originating from the helical Z15 domain. Taken together, these physical data indicate the functional attributes of the SAP sequence was preserved in Z15_EAK.

Binding of IgG to Z15_EAK

Interactions of Z15_EAK and IgG were evaluated under a non-equilibrium condition using paper chromatography (Fig.3a). Driven by capillary action, a near infrared dye conjugated antibody (IgG^{800}) carried by solvent accumulated at the point where Z15_EAK was spotted. Conversely, the EAK spot did not exhibit thee same accumulation, suggesting the interaction between IgG and Z15_EAK was not due to non-specific steric entanglement with the network fibrils. Fitting the ITC data to a two-site binding model yielded a better fit than the one-site model; for two sites, binding affinities of $2.13x10^{-6} \pm 1.07x10^{-7}$ M and $1.03x10^{-6} \pm 1.54x10^{-6}$ M were obtained (Fig. 3b). These results indicate Z15_EAK binds IgG molecules reversibly and specifically. Unlike EAK, which forms fibrils almost instantaneously upon exposure to high ionic strengths, Z15_EAK forms fibrils (Fig. 2a & 2c) slowly over 24 hours (Fig. 2b). Therefore, a co-assembly approach was used in admixing molar excess of EAK with Z15_EAK to render rapidly formed composites for capturing IgG [4, 5, 25, 26] (Fig. 4a). Integration of Z15_EAK into EAK fibrils was confirmed using SDS-PAGE electrophoresis; as the molar ratio of EAK to Z15_EAK increased, the fraction of Z15_EAK incorporated also increased (Fig. 4b). At the highest ratio tested (20:1), 58% of Z15_EAK was incorporated.

The IgG-binding function of a composite of Z15_EAK and EAK was tested in a pull-down assay in which a mixture of the peptides was found to capture a fluorescein-labeled antibody into aggregates recovered by centrifugation (Fig. 4c). The association lasted for at least 22 days *in*

vitro (Fig. S4). The equilibrium binding constant (K_d) of the composite for IgG was determined by titrating the latter against a constant concentration of the former in a microplate-based assay (Fig. 4d). Fitting the IgG and Z15_EAK/EAK data to a one-site saturation model yielded a K_d of 1.27 μM (95% CI: 0.952 μM to 1.597 μM; $R^2 = 0.9952$). Fitting the data to a two-site binding yielded ambiguous results. Titration of IgG against a constant concentration of EAK resulted in ambiguous affinity constants (data not shown), suggesting non-specific interactions. These data confirmed the IgG-binding function of Z15_EAK.

In vivo localization of IgG via Z15_EAK

To demonstrate antibody retention *in vivo*, Z15_EAK, EAK and IgG^{800} were co-injected into the posterior flank of C57BL/6 mice subcutaneously. Injection of IgG^{800} formulated with Z15_EAK and EAK (molar ratio = 1:2) remained at the injection site at levels significantly above those of IgG^{800} injected with only EAK (Fig. 5). Four days after the injection, slightly greater than 30% of the initial fluorescence intensity (FI) remained in mice received IgG^{800} admixed with Z15_EAK and EAK, whereas less than 10% of the FI remained at the injection site in mice received IgG^{800} admixed with EAK only (Fig. 5b). The FI of IgG^{800} delivered in Z15_EAK and EAK remained above background levels on day 6 and day 8, although not statistically different from FI of IgG delivered in EAK only. In mice injected with the antibody formulated in saline, the FI at the injection site was 17-fold lower on day 4 compared to that in mice received the composite formulation (Fig. S1a). The advantage in retention was also observed in the peritoneal cavity (Fig. S1b) and in footpads (Fig. S1c). These results show that the composite of Z15_EAK and EAK can be used to display Fc-binding sites in living systems.

Modeling free IgG fraction at injection depot

The effects of Z15_EAK on the kinetics of IgG retention *in vivo* was also monitored for 28 days in mouse footpads in which the materials were restricted in a confined subcutaneous space conducive for a more accurate FI measurement (Fig. 6). Each mouse was injected in one footpad with IgG^{800} formulated with EAK or a mixture of Z15_EAK and EAK. Images were captured every two days with the FI normalized to the background area on the same mouse. Consistent with the flank injection, the antibody was retained for longer durations in footpads with the inclusion of Z15_EAK and EAK compared to those injected with only EAK in the formulation. The FI was reduced to near background level between day 16 and day 18 in mice received IgG^{800} and EAK, whereas signals from the antibody delivered in a mixture of Z15_EAK and EAK remained detectable on day 28, at which point the FI measured *ex vivo* was 5.3-fold higher compared to the EAK formulation (Fig. S2). The antibody was found in the draining lymph node in the EAK mixture but not in in the Z15_EAK/EAK composite, suggesting a restricted lymphatic distribution of the latter formulation.

To estimate the fraction of free antibody in the footpads, the loss of FI was fit to a model with the injection site volume (50 µl) as the only compartment (Fig. 7a). The unbound fraction in the depot is an important consideration for antibody biotherapeutics that depend on antibody-dependent cellular cytotoxicity (ADCC) and/or complement-dependent (CDC) cytotoxicity for therapeutic benefits [27, 28]. In simulations performed in Matlab, the components injected initially appeared as a complex (Ab_Z15_EAK) in the footpad (compartment depot), which subsequently dissociating into free antibody (Ab) and the composite (Z15_EAK/EAK). Because Z15_EAK/EAK exist as supramolecular structures, only Ab was allowed to escape the depot in the

simulations. The kinetic constants k_{on} and k_{off} governing the fractions of bound and unbound (free) Ab at any given time were generated by fitting the dose concentration to a first-order process (Fig. 7b). K_d was set initially at 10^{-6} M, based on the values of one-site binding obtained *in vitro* in the microplate and ITC experiments. Estimated K_d, k_{on}, and k_{off} were then used to simulate the fractions of the species in the depot, namely the intact complex injected (Ab_Z15EAK), the composite without the antibody (Z15_EAK/EAK), and free antibody (Ab). Results of the simulations show an initial rise of free Ab peaked on day three followed by a bi-phasic decline to background on day 15, a profile mirrored the accumulation of Z15_EAK in the depot (Fig. 7c). Calculations of the relative exposures (AUC) indicate 0.27 fraction of the antibody injected existed as unbound during the 28-day period.

The impact of the dose injected on free Ab in the depot followed a non-linear trajectory; doubling the dose (2X) essentially doubled the free Ab concentration, while increasing the dose ten times (10X) only rendered a 6.9-fold increase. These correspond to 0.21 (2X) and 0.11 (10X) fractions of total Ab injected as a complex (Ab_Z15EAK). Conversely, reducing the dose by half and 10X would yield 0.31 and 0.37 fractions of free Ab, respectively (Fig. S3b). Thus, decreasing the dose would increase the free Ab fraction, while increasing the dose would lead to a decline of the free Ab fraction. The effect of dosing was also examined by simulating repeated injections. Repeating the original dose one time generated outcomes that depend on the interval (Fig. S3c). The free Ab fraction increased from 0.27 to 0.295 when the second injection were to be given on the second day. No gain in free Ab fraction was predicted if the two doses were given apart by more than 7 days. The effects of varying dose and interval could be attributed to the rapid elimination of free Ab from the depot, and the increase in Fc-binding sites due to

accumulation of Z15_EAK/EAK. These simulations provided the dosing boundary within which the fraction of free Ab could be tuned.

Inflammatory and antigenic potential

The potential of Z15_EAK to elicit inflammatory reactions was examined *in vitro* and *in vivo* (Fig. 8). Splenocytes isolated from naïve mice were cultured with 1 μg or 10 μg of Z15_EAK for 24 h and tested for production of IL-6, a pro-inflammatory cytokine produced by activated macrophages and other leukocytes in peri-implant tissues [29]. The cytokine was not detectable in the cultures except in splenocytes spiked with LPS *in vitro* (Fig. 8a). In separate experiments, splenocytes were collected from mice injected with Z15_EAK in footpads and tested for IL-6 and TNF-α production *ex vivo* on day 1, 7 and 11 after the injection (Fig. 8b & 8c) [30]. None of the mice had splenocytes produced detectable levels of IL-6 or TNF-α. No signs of irritation or swelling were observed in mice received Z15_EAK, as the footpads remained essentially the same thickness throughout the experimental period (Fig. 8 caption). No weight loss was observed in mice received Z15_EAK (data not shown). These results show that Z15_EAK did not trigger innate immunity in inducing acute or protracted inflammation.

While Z15 immunogenicity could only be determined definitively in human studies, the relatively low molecular weight led us to predict that the peptide would exhibit a reduced antigenic scope. To this end, Immune Epitope Database (IEDB) was used to predict class I and class II MHC ligands in Z15 restricted by more than 100 frequently found HLA A, B, DR, DQ, and DP alleles, covering more than 97% of the population [31-33]. Repeated administrations of the SpA-derived proteins could act as molecular mimicries, reactivating antigen-specific T cells

primed by common microbes [34]. Such restimulation by exogenous peptides could in turn stimulate effector T and B cells in humans. Using IEDB the SpA B domain sequence (B55) was found to contain a fragment resembling an HLA-A*0201-restricted T cell epitope derived from the human polyomavirus [35]. T cells of patients exposed to the virus recalled *in vitro* the peptide RIPLPNLNEDLTCGN derived from the polyomavirus 2 protein [35] (Table I). The overlapping fragment PNLNEE, conserved in B55, Z38 and Z34c, was found in the proteins' peptides predicted to be presented by multiple HLA-A alleles at affinity ranks within the 20th percentile. This potential cross-reactive sequence, discovered *post hoc*, was eliminated by the miniaturization in Z15 (Table 1 and Fig. 1a). This analysis could be a first step in a de-immunization program for peptide-based biomaterials.

While identification of cross-reactive immunogenic sequences would depend on available human data, the antigenic potential of Z15 could be assessed based on the established informatics developed for vaccine design [36]. A further risk assessment was to determine the extent to which the same regions in a given polypeptide are presented by both MHC-I and MHC-II could capture the scope of the protein's antigenic potential. Scatter analysis of MHC-I and MHC-II ligands revealed a step-wise decrease in the number of sequences dually presented by class I and class II MHC the alleles; within the 20th percentile, there were 4,227 sequences found in B55, 1,923 in Z38, 1,186 in Z34c, and 449 in Z15. The strongest binding peptides in B55 for MHC-I and MHC-II alleles were found to be 8.15 (HLA-B*15:01 and HLA-B*51:01) and 0.46 (HLA-DRB1*11:01), respectively. B55 is predicted extensively presented by class II alleles, with 202 sequences presented within the one percentile. In contrast, the strongest binding affinities predicted for Z15 were, 3.05 (HLA-B*44:02) and 2.44 (HLA-DRB5*01:01). Appending EAK

to Z15 via the GGGGS linker generated new ligands that were absent in either peptide (Fig. 9f). The Z15_EAK sequence yielded 976 ligands within the 20th percentile, with the highest affinities for class I and class II at 2.8 (HLA-A*11:01) and 2.37 (HLA-DQA1*04:01/DQB1*04:02) percentiles, respectively. The narrowing of the antigenic scope from the SpA B domain to Z15 suggests the latter might exhibit low immunogenicity in humans, although the risk can only be resolved through clinical studies.

Discussion

Herein we described an injectable, affinity-based peptide coacervate with reduced antigenic potential in Z15_EAK (Fig. 1). Spectroscopic and microscopic studies indicate that Z15_EAK oligomerized into fibrils independent of EAK (Fig. 2). The Fc-binding function of the fusion peptide was confirmed using four different methods (Fig. 3 and 4). Titration of IgG against Z15_EAK indicates their interaction was specific and reversible, with calculated K_d in the low micromolar range (Fig. 3b and 4d). In the composite, the density of the Fc-binding domain could be tuned by admixing Z15_EAK with different molar ratios of EAK (Fig. 4b), thereby providing a mechanism by which avidity of capturing IgG could be tailored for specific applications. Therefore, rather than trapping IgG through entanglements with polymer fibers, the current design allowing loading of the macromolecule via an affinity mechanism by which the release kinetics can be controlled.

An unexpected observation was self-assembly of Z15_EAK into coacervates, albeit at a slower kinetics than EAK (Fig. 2b). The kinetics of β-fibrillization occurs as a function of structural and environmental factors. The driving force of EAK fibrillization is the stacking of β-sheets as

a function of the hydrophobic interaction between inter-sheet alanine residues and charge pairing of the ionized side chains. Fibril elongation thus depends on the ionic strength of the aqueous solvent in screening charge repulsions among misaligned lysine and glutamate side chains at the interface of the β-sheets [37]. The highly regular self-complementarity of EAK strands/sheets is likely the reason for its rapid fibrillization. In case of Z15_EAK, the complementarity is diminished by the steric hindrance of the Z15 domain, causing mispairing of lysine and glutamate residues between the β-sheets. The lag time might result from re-arrangement of the β-sheets, thus slowing elongation of the fibrils. Formation of a cross-linking networking in the coacervates is a function of the length and density of the fibrils.

The Fc-binding domain was shown to be operative *in vivo*, as IgG injected with Z15_EAK and EAK was shown to localize at the injection site for extended durations (Fig. 5 and 6, and Fig. S1). The fraction of free antibody (Ab) at the injection site, a critical parameter for the pharmacodynamics of Fc-dependent biotherapeutics, was simulated computationally using a one-compartmental model (Fig. 7). While the simulations suggest dose and interval have limited impacts on the free antibody fraction, changing the kinetic constants k_{on} and k_{off} could alter the outcomes in a more dramatic manner. The latter, however, would require employing a different Fc-affinity domain. No signs of acute or protracted inflammation were observed in mice that received Z15_EAK (Fig. 8). Taken together, the data support the notion of using Z15_EAK as an injectable biomaterials platform for local deposition of antibody therapeutics *in vivo*.

Because the system consists of multiple Fc-binding sites, IgG with different specificities can be clustered in a multivalent and multifunctional fashion. The affinity-controlled mechanism allows

loading of high doses of IgG into a subcutaneous depot [38]. The drug release kinetics can be controlled by tuning the ratio of binding sites to the bioactive protein. Despite containing only one of three helices in the native Fc-binding domain, Z15_EAK exhibited specific binding to IgG, albeit at a reduced affinity. It is possible that Z15_EAK interacts with IgG at two (or more) binding sites; crystal and solution structures of SpA complexed with IgG have shown Fab as a binding site [19]. However, fitting of the binding data to a two-site model yielded ambiguous results. Nevertheless, the extended *in vivo* capture of IgG was likely due to the congregation of multiple Z15 domains in close proximity in the EAK fibrils, thereby increasing the avidity (apparent binding affinity) of the interaction, overcoming the micromolar binding affinity.

The system was shown to be non-inflammatory in the short term, but eventually the materials would be resorbed through internalization by phagocytic cells and undergo proteolytic cleavage and antigen presentation [22]. For peptide-based materials, the presentation could funnel potential immunogenic sequences to the antigen presenting machinery. Evaluation of the risk of immunogenicity requires the knowledge of the ligands' reactivity toward human T cell repertories in the context of MHC, both of which depend on individual patients. At the preclinical stage, a preliminary step would be to focus on MHC ligands that might cross-recognize by antigen-primed T cells. This was examined in IEDB querying known T cell epitopes in bacterial and viral antigens commonly found in humans. Potential T cell epitope mimicries detected in the sequences of SpA-B55, Z38, and Z34c were absent in Z15 (Fig. 1a). The elimination of the potential CD8 T cell epitope fragment PNLNE*E* was discovered *post hoc*.

For *a prior* prediction, relative scope of MHC ligands was considered. As expected, the relatively small construct Z15 was predicted to contain fewer MHC ligands than the parent Z34c protein, and its precursors (data not shown), suggesting a progressive reduction in antigenic potential. An additional analysis was conducted by tallying sequences that could be presented by both class I and class II MHC alleles. In this analysis, fewer high affinity MHC ligands were predicted to be presented dually by class I and II alleles; the extent of ligands presented by both MHC-I and MHC-II alleles decreased by close to 10-fold. Because the sets of 100+ HLA alleles analyzed covered the most of the world populations [31, 32], the results represented a reasonable estimation of the antigenic potential of Z15 in humans. Therefore we predict that the potential for Z15_EAK to elicit de novo CD4 T cell responses is relatively low. It should be noted that the miniaturization scheme was aimed to reduce the relative scope of antigenic potential, as opposed to immunogenicity, which requires human testing for definitive resolution. The approach described herein is a form of de-risking strategy.

The combined analysis of overlapping MHC-I/MHC-II ligands and known T cell epitopes described could be used to identify hotspots in SAP sequences for developing *in vitro* assays for evaluating immunogenicity in clinical studies. The development of anti-drug (materials) antibodies has been correlated with the abundance of CD4 epitopes in a given biologic. The utility of the affinity design is to minimize the number of injections needed to achieve a given local drug concentration. Particular attention should be given to the junction of Z15 and EAK because neo-antigen may be generated by such fusion. It should be noted that even endogenous proteins carry immunogenic risks [39], for example insulin [40] and anti-TNFα monoclonal antibodies [41]. In addition, the immune reactions would depend on the individual genetic

background, including HLA alleles, and the contexts in which the peptide materials are presented, for example, release of inflammatory mediators as danger signals [42]. Therefore, T-cell recognition *per se* does not necessarily preclude the development of a given SAP.

Acknowledgements

This work was supported in part by grants from the National Institutes of Health (R01 AI123392 to YF) and the Department of Defense (W81XWH1810644 to WSM). We are grateful to Dr. John Stolz for assistance with acquisition of the TEM images. We thank Dr. Javier Seravalli at the Spectroscopy and Biophysics Core for performing the calorimetric measurements.

Table I: Antigenic potential of SpA-B, Z38, Z34c, Z15, and Z15_EAK

	Region overlapping with a known T cell epitope (underlined)[#]	Number of MHC I x II sequences	Highest affinities MHC I and MHC II sequences
SpA-B	HLPNLNEEQR	4,227	8.15, 0.46
Z38	HDPNLNEEQR	1,923	5.5, 2.33
Z34c	HDPNLNEEQR	1,186	2.55, 3.51
Z15	HD----------	449	3.05, 2.44
Z15_EAK	HDGGGGSAEA	976	2.8, 2.37

[#]Class I ligands of multiple HLA-A alleles containing a fragment with linear homology with RIPLPNLNE*D*LTCGN, a peptide found to stimulate CD8 T cells from humans exposed to the human polyomavirus 2 protein restricted by HLA-A*0201 [35]

Figures and captions

Figure 1

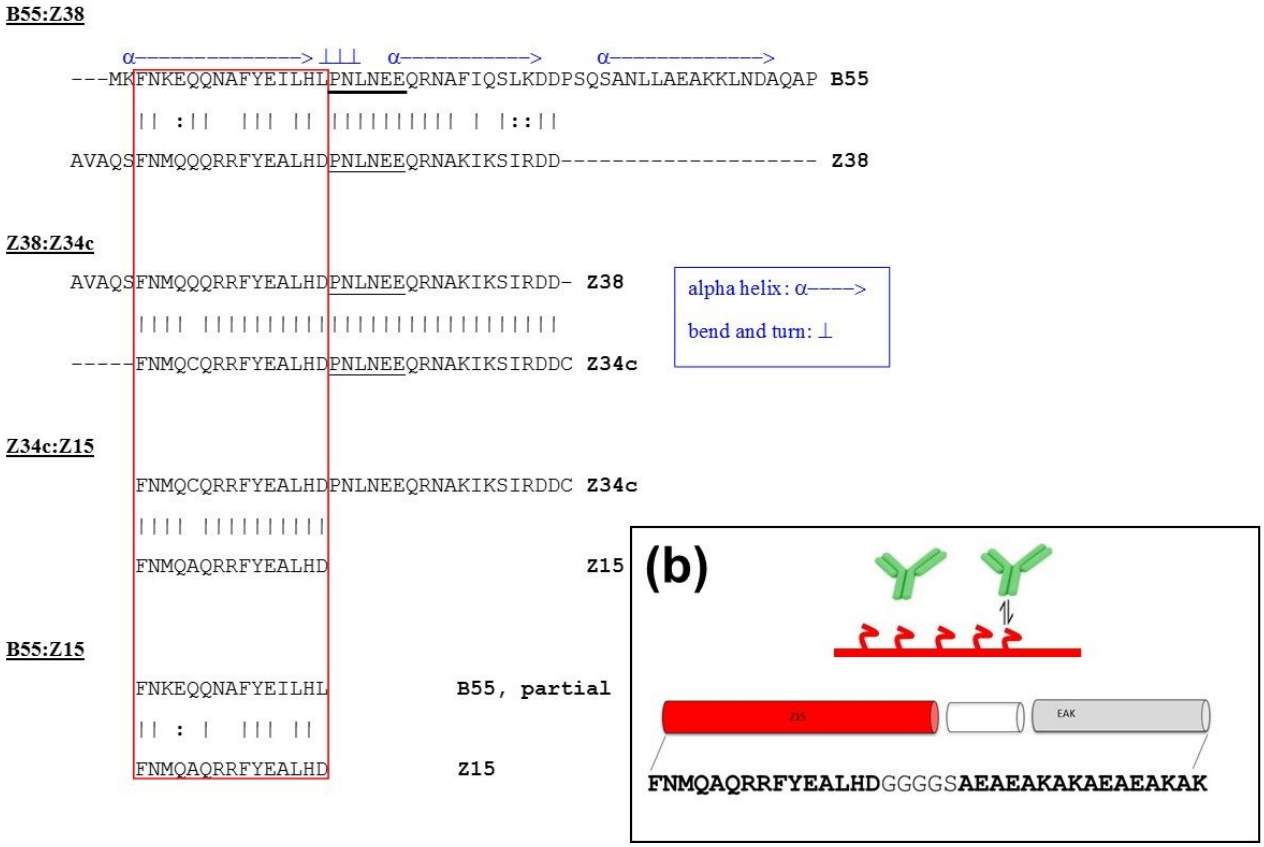

Figure 1: Design of Z15_EAK. (a) Sequence alignment of precursors of Z15, with SpA B55 and Z38, Z38, and Z34c, and lastly between the segment of B55 aligned with Z15; (b) amino acids sequence of Z15 and EAK fusion peptide. The Fc-binding domain Z15 and SAP sequence are connected through a glycine-serine tract linker.

Figure 2

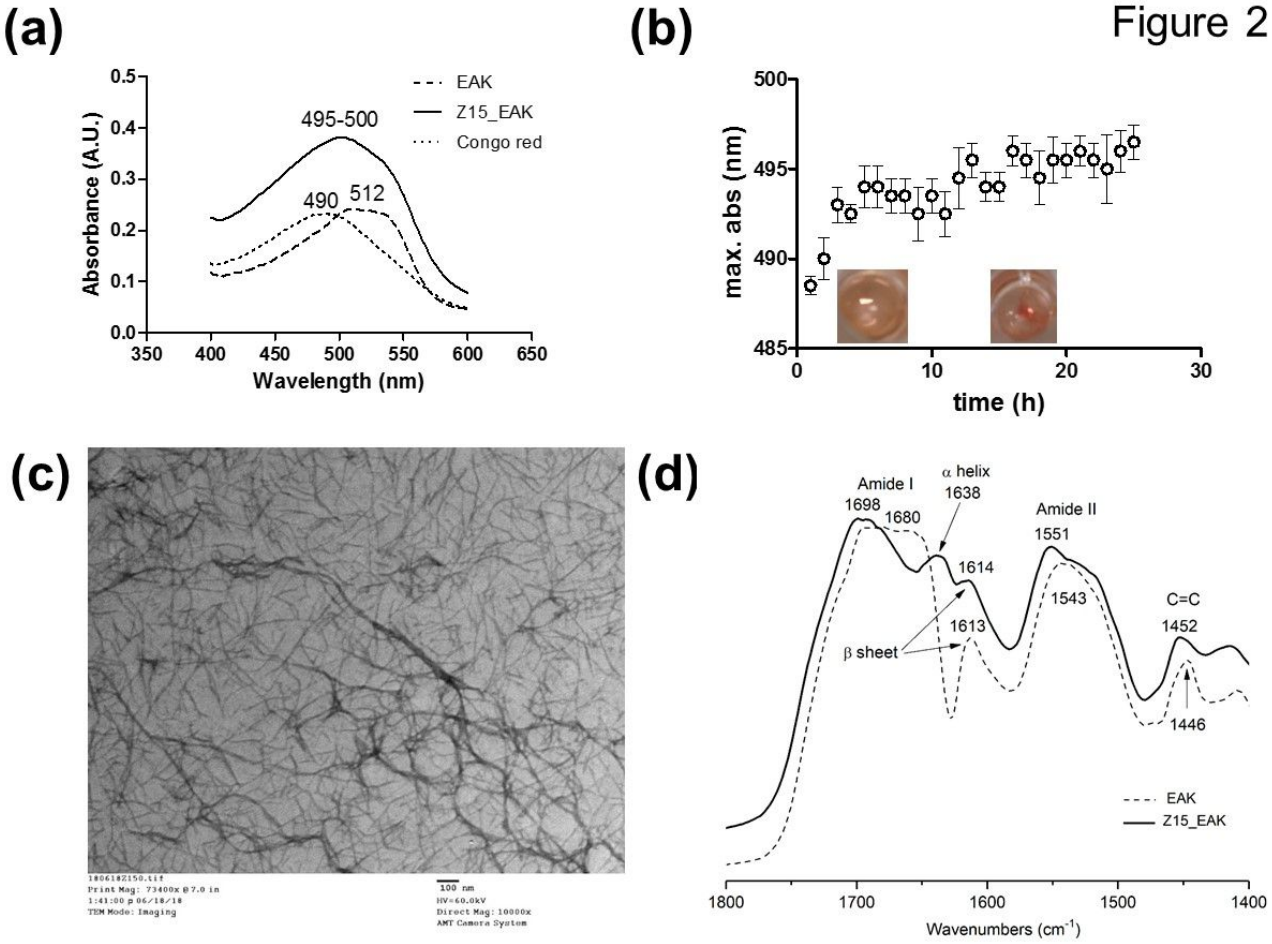

Figure 2: Physical properties of Z15_EAK. (a) Congo red spectra of Z15_EAK and EAK in phosphate buffer; (b) Congo red absorbance peaks in Z15_EAK samples over time; (c) TEM image of Z15_EAK in PBS; image was obtained at 10000x magnification. Fibrils were analyzed for widths and lengths using ImageJ; (d) FITR spectra of Z15_EAK and EAK. Each peptide and a water background control were distributed on separate steel squares and evaporated overnight. The spectra were collected from 1024 scans with DRIFT mode, baselined and presented in absorbance mode.

Figure 3

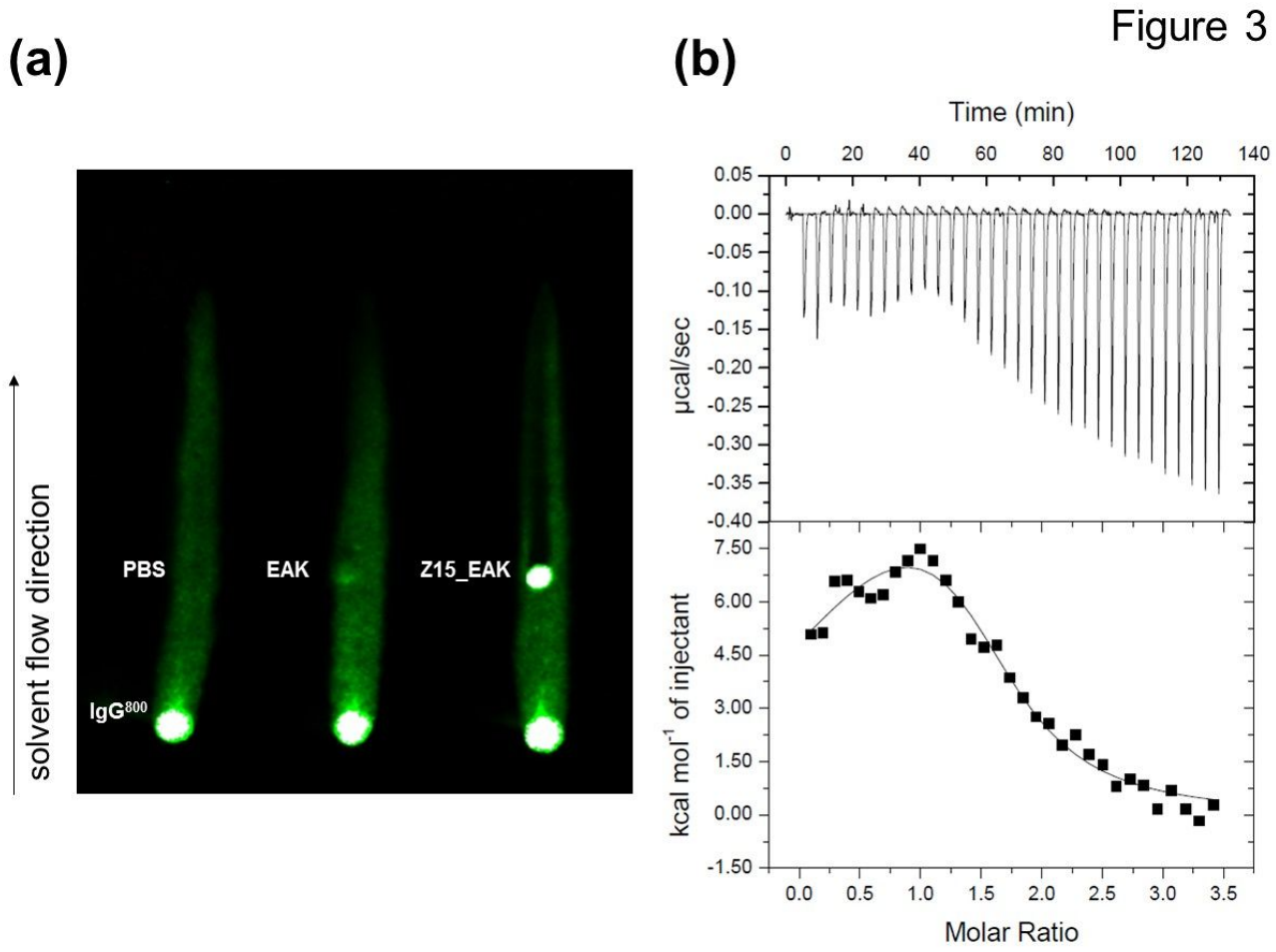

Figure 3: Binding of IgG to Z15_EAK. (a) Capture of an antibody conjugated with a near infrared dye (IgG^{800}) by Z15_EAK under a non-equilibrium condition; the antibody introduced in a Whatman paper 1 cm above the solvent. Movement of the antibody was driven by capillary action passing through EAK or Z15_EAK spotted at 6 cm offset from the bottom. (b) ITC measurement of Z15_EAK (128 µM) and IgG (8.33 µM) affinity with data fit to two-site saturation binding model.

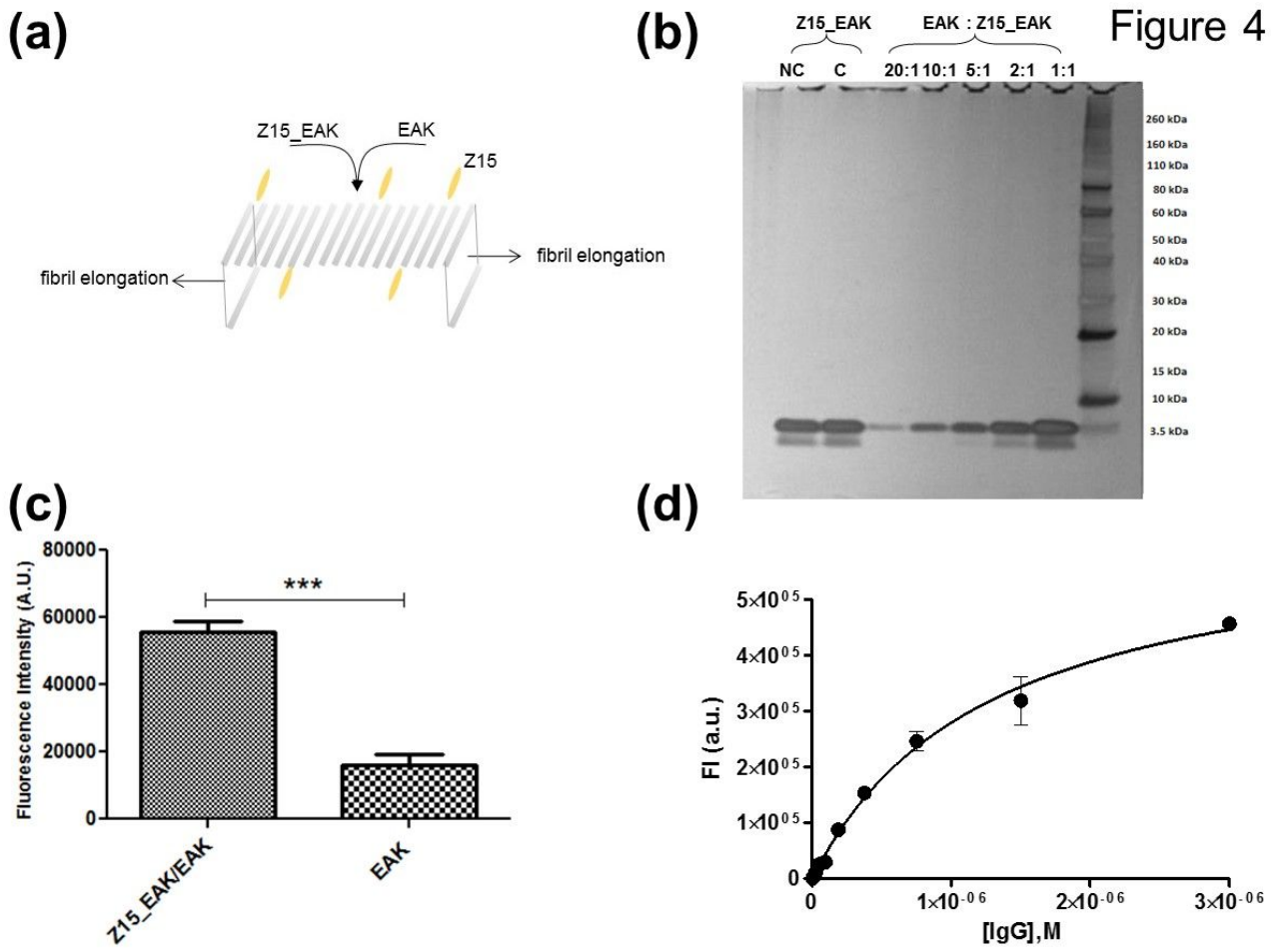

Figure 4

Figure 4: Co-assembling and binding of IgG to Z15_EAK/EAK composites. (a) Schematic of admixing Z15_EAK and EAK to attain a stable composite; (b) Denaturing SDS-PAGE electrophoretic analysis of unincorporated fraction of Z15_EAK in the mixture of EAK and Z15_EAK at 20:1, 10:1, 5:1, 2:1, and 1:1. Lane intensities were quantified using ImageJ with the percent captured determined based on the average intensities of non-centrifuged ("NC") and centrifuged ("C") Z15_EAK bands. Percent Z15_EAK captured of 20:1, 10:1, 5:1, 2:1, and 1:1 were 58%, 23%, 16%, 13%, and 12%, respectively. (c) A pull-down assay showing co-localization of IgG^{FITC} with a mixture of Z15_EAK and EAK upon centrifugation; unpaired t-test $p<0.05$. (d) Titration of a fluorescein-labeled rabbit polyclonal IgG to Z15_EAK/EAK in a round-bottom, medium-adsorptive microplate; unbound IgG were removed by washing through

repeated centrifugation steps. Data (subtracted with background binding) were fit to one-site saturation binding.

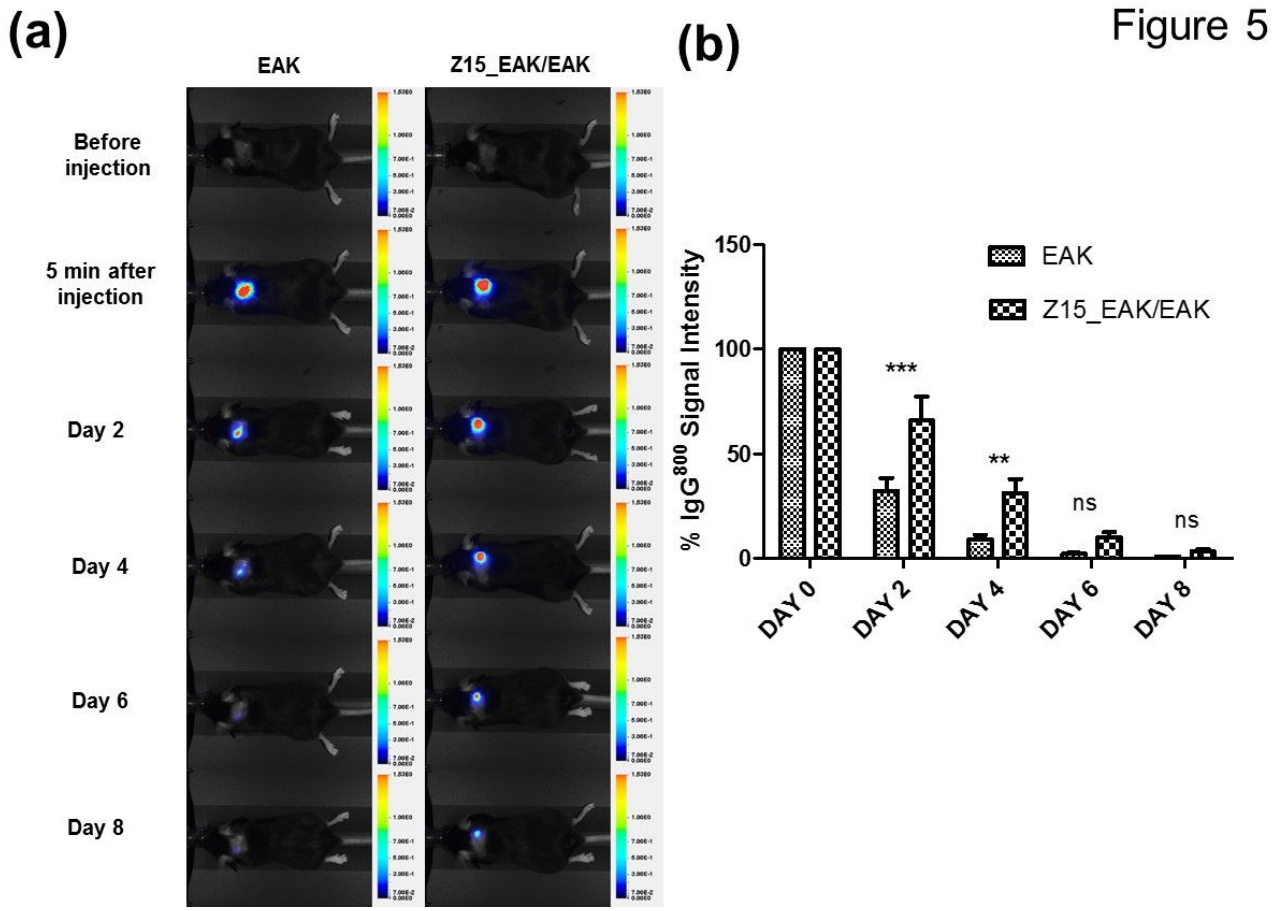

Figure 5

Figure 5: *In vivo* retention of IgG. (a) Representative images of mice injected subcutaneously with IgG^{800} formulated in EAK or Z15_EAK/EAK; all images were set to the same color scale; (b) Quantification of fluorescence intensities at the different time points (n = 8 for each group, two-way ANOVA, Bonferroni post hoc test comparing mean FI at each time point; *** $p < 0.001$, ** $p < 0.01$, ns not significant). Similar advantage was observed at with other antibody doses in different anatomical locations (supplemental Fig. S1)

Figure 6

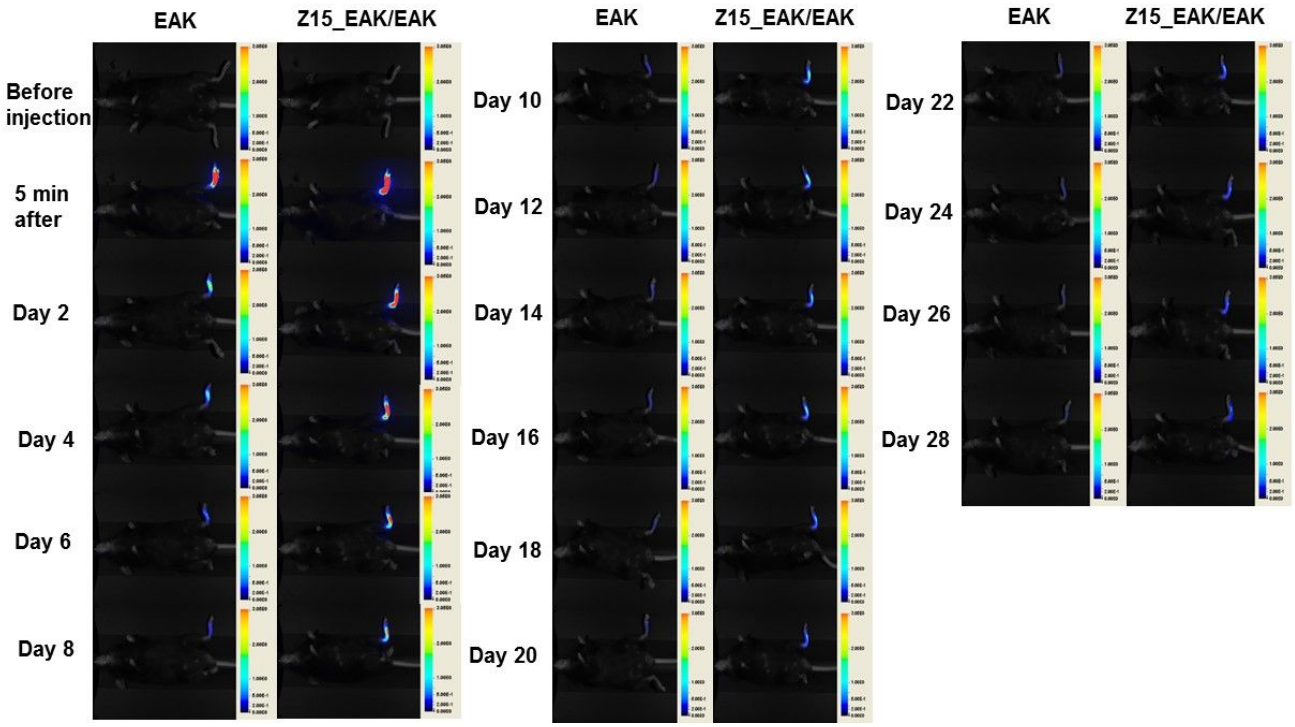

Figure 6: *In vivo* retention of IgG in footpad. Images of mice injected with IgG^{800} pre-mixed with EAK or Z15_EAK/EAK; all images were set the same color scale and resolution (255 μm); fluorescence intensities were quantified and converted to concentration or percent with the signal obtained 5 min after injection as the highest concentration or 100%. After 4 days, 34% of IgG^{800} retained in the footpad injected with Z15_EAK/EAK while only 8% retained in EAK control footpad. Difference at end point can be found in supplemental Fig. S2.

Figure 7

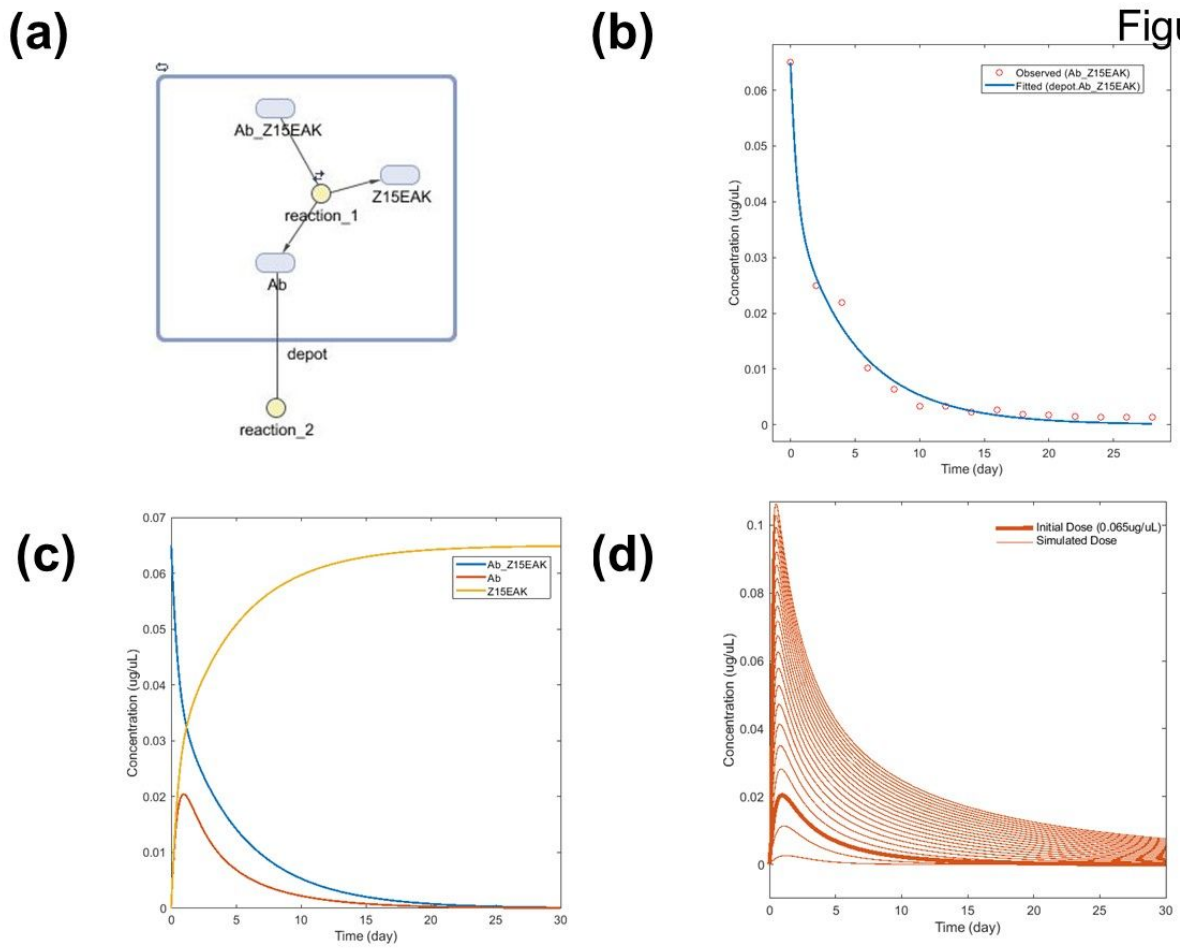

Figure 7: Simulation of antibody in footpad injection depot. (a) One-compartment model diagramed using the Matlab Simbiology module (2017a) with the simulations governed by the equations described in Methods and Materials. Since it was assumed that no other anatomical structure or physiological mechanism was involved in the clearance, the depot is the single compartment in which the gel was injected, with "Ab_Z15EAK" representing IgG^{800} complexed with Z15_EAK/EAK coacervate, "Ab" representing dissociated IgG^{800}, and "Z15EAK" representing Z15_EAK and EAK (which were assumed to remain always in the depot); reaction_1 represents reversible binding (k_{on} and k_{off}) between antibody and Z15, and reaction_2 represents elimination of antibody from the depot (k_{el}); (b) Fitting of *in vivo* decay data in Fig. 6 to first-order elimination model to obtain k_{el}; (d) Simulated profiles of the complex,

Z15_EAK/EAK composite, and free antibody using K_d determined in ITC and the microplate assay. AUC was calculated using a trapezoidal numerical integration function in Matlab.

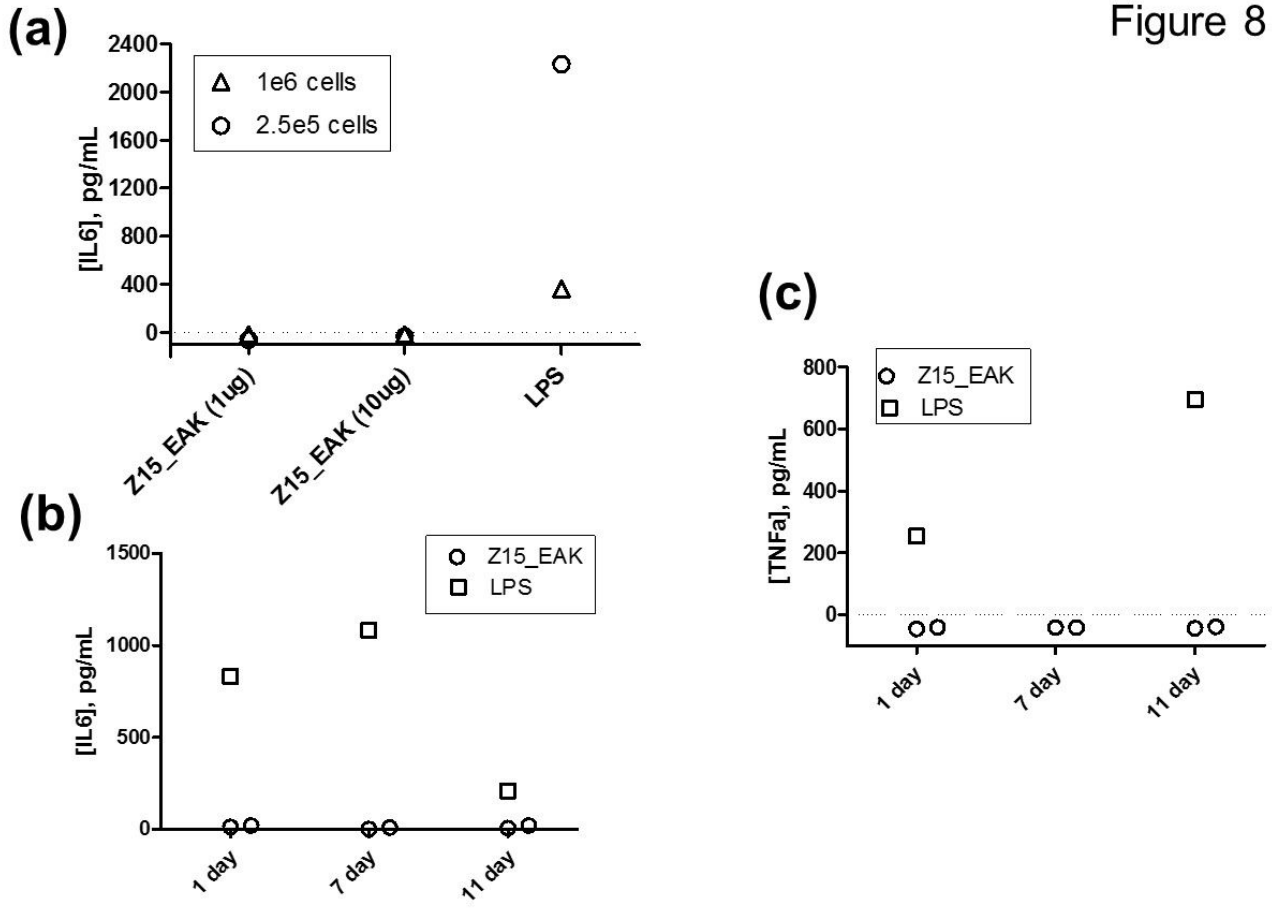

Figure 8: Analysis of pro-inflammatory cytokines produced by splenocytes in response to Z15_EAK. Cells were cultured overnight and supernatants were tested using IL-6 and TNF-α ELISA with detection limits of 15.6 pg/ml and 8 pg/ml, respectively. (a) IL-6 concentration detected from Z15_EAK exposed to naïve splenocytes at $2x10^5$ and $1x10^6$ cells per ml; (b) IL-6 concentration and (c) TNF-α concentration detected from splenocytes of Z15_EAK injected mice (n=2 for each time point). 125 µg Z15_EAK was injected to each footpad in the 1-day and 11-day experiments (each mouse received 250 µg Z15_EAK in total). In the 7-day experiment, 125

µg Z15_EAK was injected to the right footpad while the left footpad received the equivalent volume of saline to monitor the footpad thickness at 1 h and 7 days after injection. The footpad thickness (mean and standard deviation) before injection and 1h after Z15_EAK injection were 3.04 ± 0.05 mm and 3.45 ± 0.07 mm, respectively. After 7 days the thickness was 2.73 ± 0.3 mm. Injecting saline into the other footpad in mice yielded measurements of 2.5 ± 0.51 mm and 3.1 ± 0.14 cm, before and 1h after. The thickness on day 7 in the saline group measured 2.45 ± 0.09 mm.

Figure 9

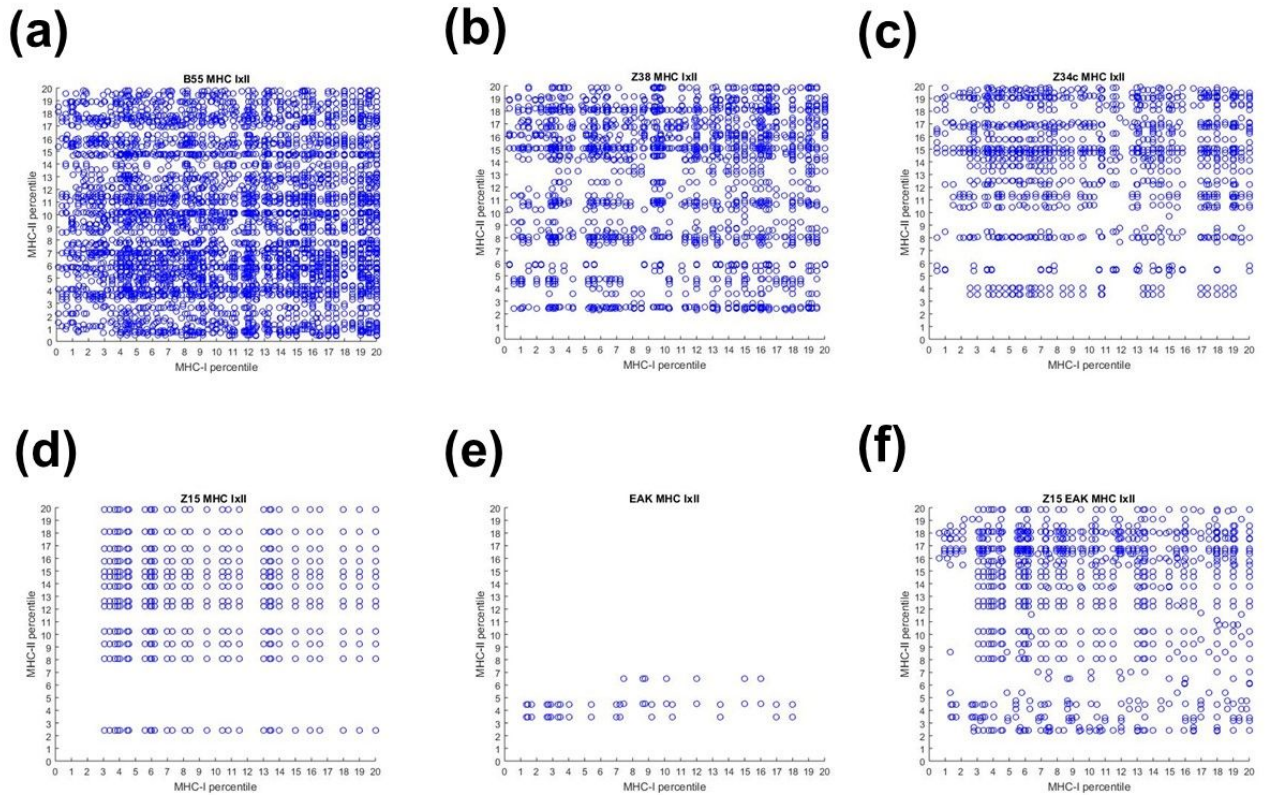

Figure 9: Analysis of overlapping ligands presented by MHC-I and MHC-II alleles. Sequences of SpA B55 (a), Z38 (b), Z34c (c), Z15 (d), EAK (e), and Z15_EAK (f) were scanned for MHC ligands using IEDB based on 100+ HLA class I and II alleles. The analysis is represented as

scatter plots of of MHC-I (x-axis) and MHC-II (y-axis) ligands in a given sequence. The density of each scatter plot suggests the extent of overlapping MHC I and MHC II ligands, thereby providing a theoretical measure of relative antigenicity. A custom Matlab script was used to scan for overlapping MHC-I and MHC-II ligands, according to their percentile ranks of binding affinities for the alleles [34].

References

1. S. Zhang, T. C. Holmes, C. M. DiPersio, R. O. Hynes, X. Su and A. Rich, *Biomaterials*, 1995, **16**, 1385-1393.
2. S. Zhang, C. Lockshin, R. Cook and A. Rich, *Biopolymers*, 1994, **34**, 663-672.
3. S. Zhang, *Nat Biotechnol*, 2003, **21**, 1171-1178.
4. Y. Zheng, Y. Wen, A. M. George, A. M. Steinbach, B. E. Phillips, N. Giannoukakis, E. S. Gawalt and W. S. Meng, *Biomaterials*, 2011, **32**, 249-257.
5. Y. Wen, S. L. Roudebush, G. A. Buckholtz, T. R. Goehring, N. Giannoukakis, E. S. Gawalt and W. S. Meng, *Biomaterials*, 2014, **35**, 5196-5205.
6. Y. Wen, W. Liu, C. Bagia, S. Zhang, M. Bai, J. M. Janjic, N. Giannoukakis, E. S. Gawalt and W. S. Meng, *Acta Biomater*, 2014, **10**, 4759-4767.
7. Y. Wen, H. R. Kolonich, K. M. Kruszewski, N. Giannoukakis, E. S. Gawalt and W. S. Meng, *Mol Pharm*, 2013, **10**, 1035-1044.
8. M. J. Saunders, W. Liu, C. Szent-Gyorgyi, Y. Wen, Z. Drennen, A. S. Waggoner and W. S. Meng, *Bioconjugate Chemistry*, 2013, **24**, 803-810.
9. W. Liu, M. J. Saunders, C. Bagia, E. C. Freeman, Y. Fan, E. S. Gawalt, A. S. Waggoner and W. S. Meng, *J Control Release*, 2016, **230**, 1-12.
10. A. Tajima, W. Liu, I. Pradhan, S. Bertera, C. Bagia, M. Trucco, W. S. Meng and Y. Fan, *Clin Immunol*, 2015, **160**, 82-89.
11. A. Tajima, W. Liu, I. Pradhan, S. Bertera, R. A. Lakomy, W. A. Rudert, M. Trucco, W. S. Meng and Y. Fan, *Journal of visualized experiments : JoVE*, 2016, DOI: 10.3791/54062.
12. M. Tashiro, R. Tejero, D. E. Zimmerman, B. Celda, B. Nilsson and G. T. Montelione, *J Mol Biol*, 1997, **272**, 573-590.
13. C. Ballow, A. Leh, K. Slentz-Kesler, J. Yan, D. Haughey and E. Bernton, *The Journal of Clinical Pharmacology*, 2013, **53**, 909-918.
14. T. Moks, L. AbrahmsÉN, B. Nilsson, U. Hellman, J. SjÖQuist and M. UhlÉN, *European Journal of Biochemistry*, 1986, **156**, 637-643.
15. J. Sjodahl, *Eur J Biochem*, 1977, **78**, 471-490.
16. B. Nilsson, T. Moks, B. Jansson, L. Abrahmsen, A. Elmblad, E. Holmgren, C. Henrichson, T. A. Jones and M. Uhlen, *Protein engineering*, 1987, **1**, 107-113.
17. J. Deisenhofer, *Biochemistry*, 1981, **20**, 2361-2370.

18. L. Jendeberg, B. Persson, R. Andersson, R. Karlsson, M. Uhlen and B. Nilsson, *Journal of molecular recognition : JMR*, 1995, **8**, 270-278.
19. H. Gouda, M. Shiraishi, H. Takahashi, K. Kato, H. Torigoe, Y. Arata and I. Shimada, *Biochemistry*, 1998, **37**, 129-136.
20. M. A. Starovasnik, A. C. Braisted and J. A. Wells, *Proceedings of the National Academy of Sciences of the United States of America*, 1997, **94**, 10080-10085.
21. A. S. Hoffman and P. S. Stayton, *Progress in Polymer Science (Oxford)*, 2007, **32**, 922-932.
22. J. D. Bryers, C. M. Giachelli and B. D. Ratner, *Biotechnology and bioengineering*, 2012, **109**, 1898-1911.
23. S. Tsonchev, K. L. Niece, G. C. Schatz, M. A. Ratner and S. I. Stupp, *J Phys Chem B*, 2008, **112**, 441-447.
24. A. C. Braisted and J. A. Wells, *Proceedings of the National Academy of Sciences of the United States of America*, 1996, **93**, 5688-5692.
25. G. A. Hudalla, T. Sun, J. Z. Gasiorowski, H. Han, Y. F. Tian, A. S. Chong and J. H. Collier, *Nature materials*, 2014.
26. J. Z. Gasiorowski and J. H. Collier, *Biomacromolecules*, 2011, **12**, 3549-3558.
27. A. Saxena and D. Wu, *Frontiers in immunology*, 2016, **7**, 580.
28. J. E. Bakema and M. van Egmond, *Current topics in microbiology and immunology*, 2014, **382**, 373-392.
29. R. Caruso, L. Botta, A. Verde, F. Milazzo, I. Vecchi, M. G. Trivella, L. Martinelli, R. Paino, M. Frigerio and O. Parodi, *PloS one*, 2014, **9**, e90802.
30. F. Javed, K. Al-Hezaimi, Z. Salameh, K. Almas and G. E. Romanos, *Cytokine*, 2011, **53**, 8-12.
31. D. Weiskopf, M. A. Angelo, E. L. de Azeredo, J. Sidney, J. A. Greenbaum, A. N. Fernando, A. Broadwater, R. V. Kolla, A. D. De Silva, A. M. de Silva, K. A. Mattia, B. J. Doranz, H. M. Grey, S. Shresta, B. Peters and A. Sette, *Proceedings of the National Academy of Sciences of the United States of America*, 2013, **110**, E2046-2053.
32. J. Greenbaum, J. Sidney, J. Chung, C. Brander, B. Peters and A. Sette, *Immunogenetics*, 2011, **63**, 325-335.
33. P. Wang, J. Sidney, Y. Kim, A. Sette, O. Lund, M. Nielsen and B. Peters, *BMC bioinformatics*, 2010, **11**, 568.
34. B. J. Andrick, A. I. Schwab, B. Cauley, L. A. O'Donnell and W. S. Meng, *PloS one*, 2015, **10**, e0135451.
35. J. Mani, L. Wang, A. G. Huckelhoven, A. Schmitt, A. Gedvilaite, N. Jin, C. Kleist, A. D. Ho and M. Schmitt, *Oncotarget*, 2017, **8**, 2485-2500.
36. W. Fleri, S. Paul, S. K. Dhanda, S. Mahajan, X. Xu, B. Peters and A. Sette, *Frontiers in immunology*, 2017, **8**, 278.
37. D. W. Urry, *Peptide Science*, 1998, **47**, 167-178.
38. L. Kagan, M. R. Turner, S. V. Balu-Iyer and D. E. Mager, *Pharm Res*, 2012, **29**, 490-499.
39. A. S. De Groot and D. W. Scott, *Trends in immunology*, 2007, **28**, 482-490.
40. R. P. Radermecker and A. J. Scheen, *Diabetes/metabolism research and reviews*, 2007, **23**, 348-355.
41. M. Svenson, P. Geborek, T. Saxne and K. Bendtzen, *Rheumatology (Oxford)*, 2007, **46**, 1828-1834.
42. P. Matzinger, *Science*, 2002, **296**, 301-305.

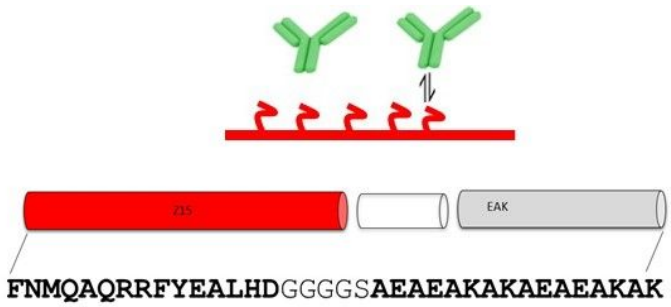

A novel bi-functional peptide consisting of an Fc-binding domain and self-assembly sequence is shown to retain IgG in vivo.